Journal of Applied Electrochemistry 30: 303–313, 2000.
© 2000 Kluwer Academic Publishers. Printed in the Netherlands.

Mass transfer between a liquid and an array of discs in a cylindrical container. Part II: Combined pumped flow and rotation

E. BEZERRA CAVALCANTI[1] and F. CŒURET[2]*

[1]*C.C.T./D.E.Q., Univ. Federal da Paraíba, Av. Aprigio Veloso 882, Bodocongó, Campina Grande 58109.000, Pb, Brazil*

[2]*Laboratoire de Thermocinétique – U.M.R. CNRS no. 6607 – Nantes, Implantation: Ecole Louis de Broglie, Campus de Ker Lann, 35170 Bruz, France*

*(*author for correspondence, e-mail: coeuret@isitem.univ-nantes.fr)*

Received 24 December 1998; accepted in revised form 13 July 1999

Key words: electrochemical method, electrochemical reactor, empirical correlations, mass transfer coefficient, radial flow, rotating disc contactor

Abstract

The work is a continuation of an electrochemical mass transfer study which employed a cell with alternatingly spaced annular and full discs. Pumped liquid flow through the cell is now combined with rotation of the full discs. The influence of the different parameters on mass transfer at four characteristic surfaces in a cell element is analysed, and an empirical correlation is obtained for each surface. In the entrance region, where the radial flow is divergent, mass transfer control is mixed, while it is controlled by rotation in the convergent exit channel.

List of symbols

A_e electrode surface area (m^2)
C_∞ concentration of ferricyanide ions (mol m^{-3})
D molecular diffusion coefficient (m^2 s^{-1})
e hydraulic radius (m)
F Faraday constant (96 500 C mol^{-1})
h half-distance between two discs (m)
H distance between two discs, $2h$ (m)
I_L limiting diffusion current (A)
$\bar{k}_d$ mean mass transfer coefficient (m s^{-1})
N rotation velocity (rpm)
Q_V volumetric flow rate (m^3 s^{-1})
R_0 radius of the full disc (m)
R_1 inner radius of the annular disc (m)
R_2 inner radius of the cell (outer radius of the annular disc) (m)
Re_C channel Reynolds number used by Jansson, $(Q_v/H\nu)$
Re_H rotational Reynolds number based on H, $(\omega H^2/\nu)$
Re_m channel Reynolds number used by Kreith, $(Q_v/(2\pi H\nu))$
Re_R rotational Reynolds number based on R, $(\omega R^2/\nu)$
Ro Rossby number, (Re_C/Re_R)
Sc Schmidt number, (ν/D)
$\overline{Sh}$ mean Sherwood number, $(2h\bar{k}_d/D)$
Ta Taylor number, $(h^2\omega/\nu)^{0.5}$

Greek symbols
β exponent
μ dynamic viscosity (kg m^{-1} s^{-1})
ν kinematic viscosity (m^2 s^{-1})
ρ density (kg m^{-3})
ω angular velocity (s^{-1})

1. Introduction

In Part I [1] mass transfer between a liquid and discs arranged in a cylindrical cell (Figure 1) was studied in the two limiting situations of pumped flow through a stationary arrangement, and rotation of the full discs. The electrochemically measured average mass transfer coefficients between the liquid and the four surfaces *1* to *4* of a modulus (Figure 1) were analysed and empirically correlated.

It is known that the space-time yield of electrochemical reactors is improved when high mass transfer coefficients at the working electrode are attained while volumetric flow rates are small [2]. This signifies that the mass transfer coefficient has to be increased by other means than the flow rate; one of the possible means is electrode rotation. This was the basic idea in the Couette–Taylor–Poiseuille electrochemical reactor [2–4], and of the 'Eco-cell' proposed for metal recovery from dilute solutions [5]. Another electrochemical reactor which combines the rotation of one electrode and forced flow, in order to obtain high space-time yields, that is, high values of the conversion per pass through a reactor having a small volume, is shown in Figure 1. In

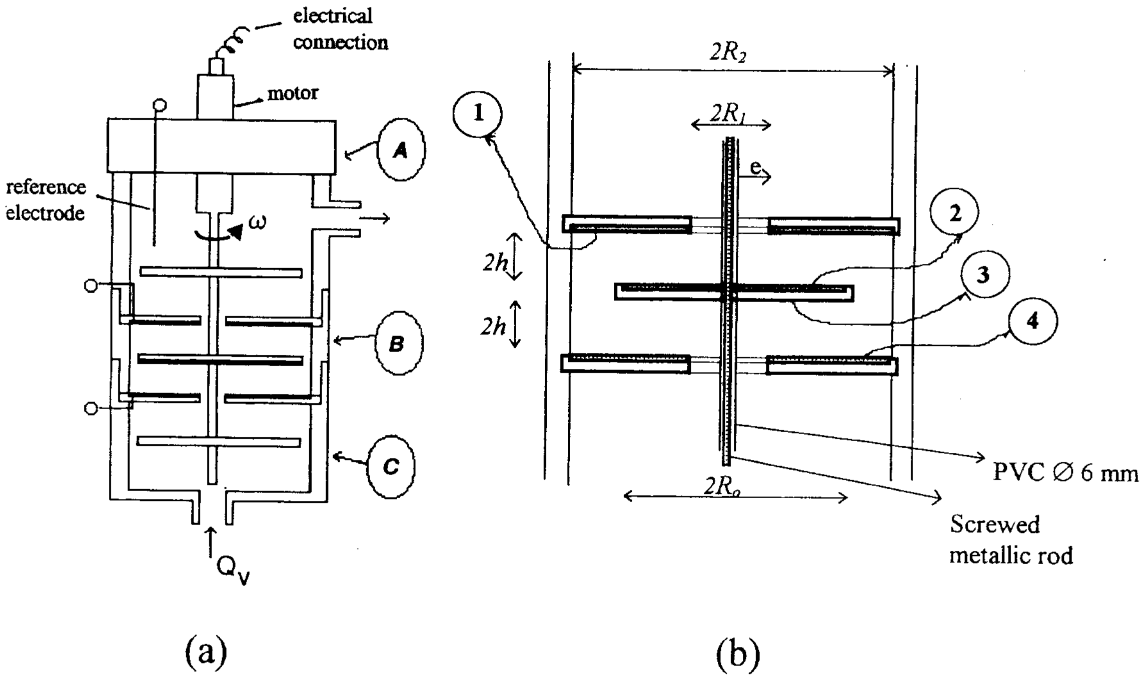

Fig. 1. Experimental cell: (a) general view; (b) view of the four surfaces in the modulus. Geometrical parameters: $2R_0 = 50$, 54 and 56 mm; $2R_1 = 12$, 16 and 20 mm; $2R_2 = 60$ mm; $2h = 2$, 4, 6 and 8 mm; $e = 3$, 5 and 7 mm.

the case of the 'pump cell', which only contains a rotating disc and a stationary disc, the flow rate is induced by rotation [6].

The present work concerns mass transfer to surfaces *1* to *4* of the cell in Figure 1 except that pumped flow is now combined with rotation of the full discs (surfaces *2*–*3*). Such an arrangement has been previously studied as a rotating-disc contactor for liquid–liquid extraction [7]. Under turbulent conditions, intense recirculation between the rotating and the stationary discs provides thorough mixing of the two phases and, creates consequently, an efficient extraction process.

2. Hydrodynamics and mass transfer from the literature

The system now considered has two limiting cases studied previously by the present authors: rotation of a disc in a closed cylinder [8] and pumped liquid flow alone between stationary discs [1].

The flow structure resulting from the combination of a pumped flow with the rotation of a disc opposite to a stationary disc was studied by several authors, especially in the case of single phase fluids. Recirculation is generated in the interdisc space, as a result of the fact that the rotating disc puts energy into the fluid by moving it towards the periphery, while energy is dissipated on the stationary disc [7]. The modification suffered by the flow structure depends on the radial flow direction between the discs (inflow or outflow). The works of Adams and Szeri [9], Szeri [10], Prakash [11], Thomas [12] and Peres [13] were devoted to such a complex flow, the study of which lies beyond the scope of our work. To estimate which mode exerts predominant influence, the channel Reynolds number, Re_C, and the rotation Reynolds number, Re_R, are combined in the Rossby number $R_0 = Re_C/Re_R$ [10].

Average mass transfer rates between a fluid and the discs, in the presence of forced flow were studied by the groups of Kreith and Jansson. Based on measurements using the naphthalene dissolution method, Kreith [14] proposed an empirical correlation for mass transfer between a flowing gas and a rotating disc: the Sherwood number was expressed as function of the rotation Reynolds number, Re_R, and the channel Reynolds number, $Re_m = Re_C/(2\pi)$. The research team of Jansson determined electrochemically mass transfer coefficients in view of the development of the pump cell. Jansson and Ashworth [15] proposed empirical correlations of the type $\overline{Sh} = f(Re_C; Re_R$; geometrical parameters) for the rotating and the fixed disc. They observed that channel flow is dominant when $Re_C/Re_R > 1$; they also measured distributions of local mass transfer coefficients over the discs, showing an entry effect. Their study was continued by Jansson and Marshall [16], and also by Groroghchian et al. [17] who considered a convergent flow (or inflow) and proposed empirical correlations giving the average Sherwood number, together with experimental distributions of local mass transfer coefficients.

The empirical mass transfer correlations corresponding to exchange surfaces (in bold), and the domains of validity of the correlations, are summarized in Table 1. The lack of lateral confinement in the systems employed by the authors of these correlations, provided interest for experimental work presented here.

Table 1. Empirical correlations for wall-to-liquid mass transfer (combined flow rate and rotation)

Authors	Correlation	Domain of validity	System and surface	Method
Kreith et al. [14]	$\overline{Sh} = \left(\frac{h}{R_2}\right)^{0.55} \left[\begin{array}{l} 1.36 + 1.29 \times 10^{-5} Re_R + 3.57 \times 10^{-10} Re_R^2 \\ -3.51 \times 10^{-15} Re_R^3 + 1.84 \times 10^{-20} Re_R^4 \end{array}\right] \times \left[Re_m^{[0.83 - 12 \times 10^{-4} Re_R]}\right]$	$Sc = 2.4$ $0 < Re_R < 4 \times 10^4$ $5 \times 10^3 < Re_m < 1 \times 10^5$ $0.12 < 2h/R_2 < 0.6$	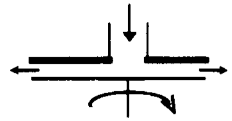	Dissolution
Jansson and Ashworth [15]	$\overline{Sh} = 1.56 \times 10^{-3} \left(Re_C \frac{H}{R_2} Re_R \frac{H^2}{R_2^2 - R_1^2}\right)^{0.6}$	$Sc = 840$ $8 \times 10^{-4} < 2h/R_2 < 9 \times 10^{-3}$ $7 \times 10^5 < Re_R < 1.5 \times 10^6$	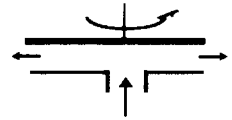	Electrochemical
	$\overline{Sh} = 5.6 \times 10^{-3} \left(Re_C \frac{H}{R_2} Re_R \frac{H^2}{R_2^2 - R_1^2}\right)^{0.5}$		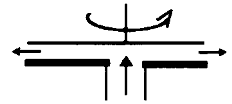	
Groroghchian et al. [17]	$\overline{Sh} = 4.9 \left(Re_R \frac{h^2}{R_2^2 - R_1^2}\right)^{0.57} Sc^{1/3}$ $\overline{Sh} = 4 \times 10^{-3} Sc^{1/3} Re_m^{0.1} Re_R^{0.57}$	$4.7 \times 10^4 < Re_R < 1.5 \times 10^5$ $3 \times 10^4 < Re_C < 13 \times 10^4$ $2h/R_2 = 0.025$ $Re_R < 4.7 \times 10^4$	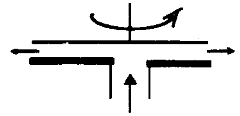	Electrochemical
Present work	$\overline{Sh} = 1.19\ Re_C^{0.07} Re_R^{0.43} \left(\frac{H^2}{R_2^2 - R_1^2}\right)^{0.35} Sc^{1/3}$	$395 < Re_C < 2.3 \times 10^4$ $3.5 \times 10^3 < Re_R < 8.7 \times 10^4$ $4.6 \times 10^{-3} < 2h/R_2 < 0.074$	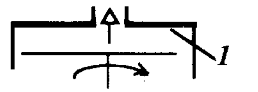	Electrochemical
	$\overline{Sh} = 0.35\ Re_C^{0.14} Re_R^{0.4} \left(\frac{H^2}{R_2^2 - R_1^2}\right)^{0.38} Sc^{1/3}$		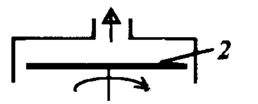	
	$\overline{Sh} = 1.58 (Re_C Re_R)^{0.26} \left(\frac{H^2}{R_2^2 - R_1^2}\right)^{0.69} Sc^{1/3}$		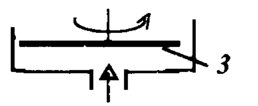	
	$\overline{Sh} = 0.2 \left(Re_C Re_R \frac{H^2}{R_2^2 - R_1^2}\right)^{0.27} Sc^{1/3}$		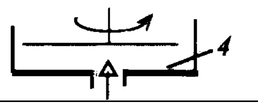	

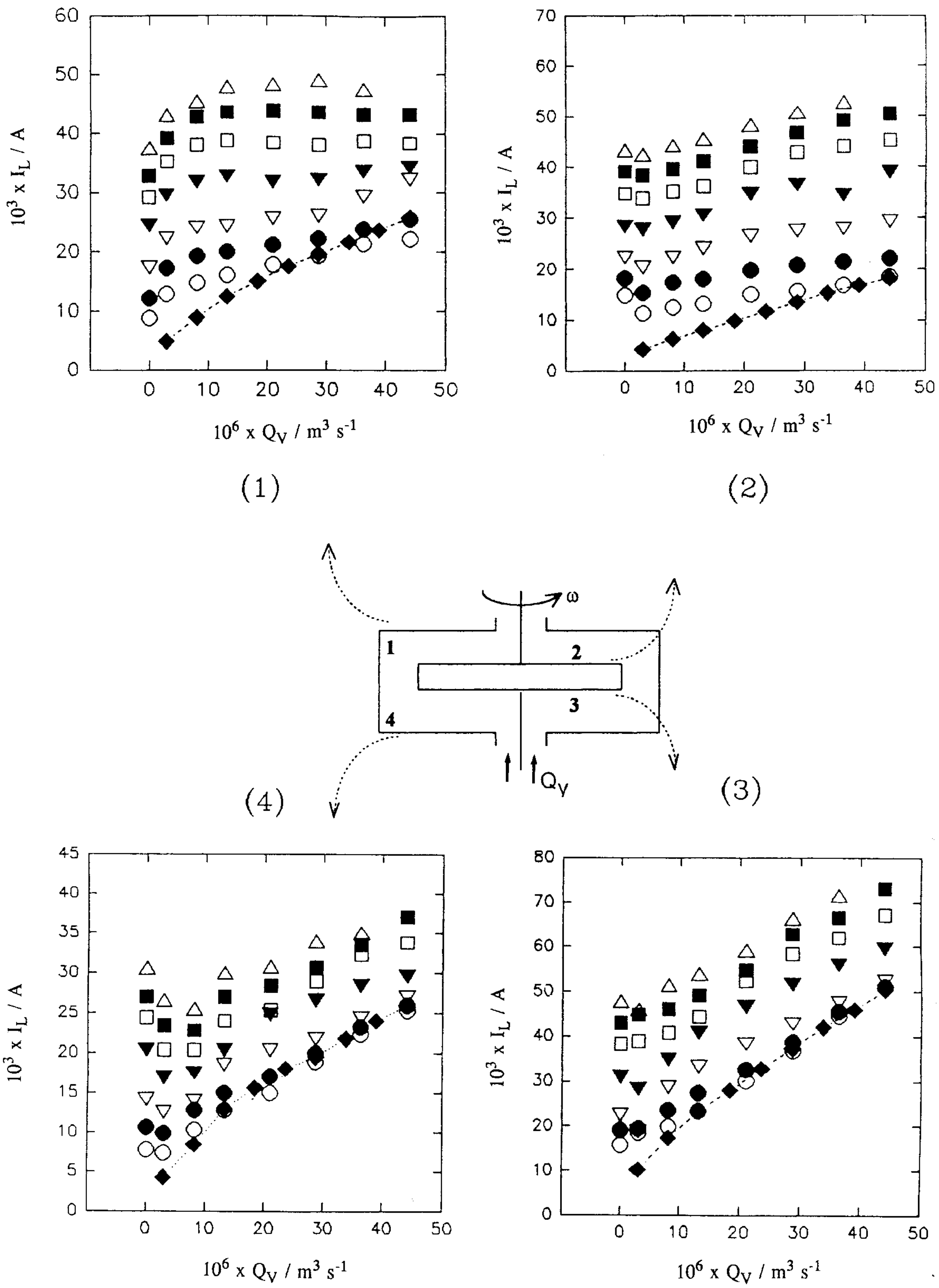

Fig. 2. Mass transfer to surfaces *1* to *4*: variation of I_L with Q_V at constant N (for $2h = 8$ mm; $2R_1 = 12$ mm). Key for N: (◆) 0, (○) 50, (●) 100, (▽) 200, (▼) 400, (□) 600, (■) 800 and (△) 1000 rpm.

The recirculation cell considered in [8] is altered when there is a supporting rotating rod in the space between the two discs [1]. The addition of pumped flow will interfere with rotation and lead to a modified flow structure; mass transfer at surfaces *1* to *4* could be distinctly affected by the combination of forced flow and rotation.

3. Experimental results

The cell and the geometrical parameters (Figure 1), the experimental method (electrochemical reduction of ferricyanide), and the experimental details, were the same as in Part I [1]. The mean mass transfer coefficient,

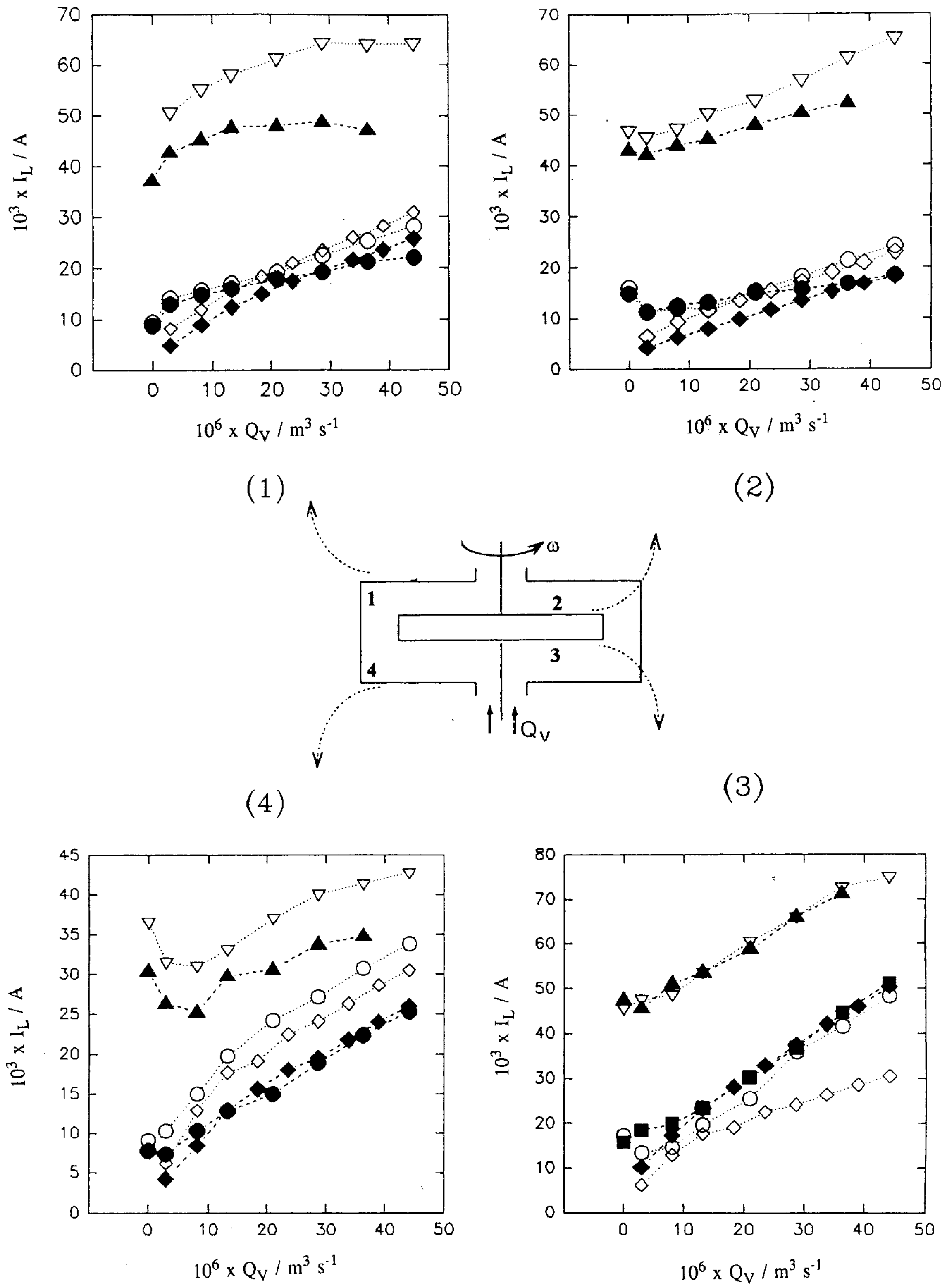

Fig. 3. Mass transfer to surfaces *1* to *4*: variation of I_L with Q_V at constant N (for $2h = 4$ mm and 8 mm; $2R_1 = 12$ mm). Key for N: (◆) 0, (■) 50 and (▲) 1000 rpm at $2h = 8$ mm; (◇) 0, (○) 50 and (▽) 1000 rpm at $2h = 4$ mm.

$\bar{k}_d$, was calculated from the measured limiting diffusion current, I_L, according to the following expression:

$$\bar{k}_d = \frac{I_L}{FA_eC_\infty}$$

where F is the faradaic constant, A_e the area of the transfer surface (cathode) and C_∞ the concentration of ferricyanide ions.

In each Figure showing experimental results, a small diagram of the elementary cell indicates the correspon-

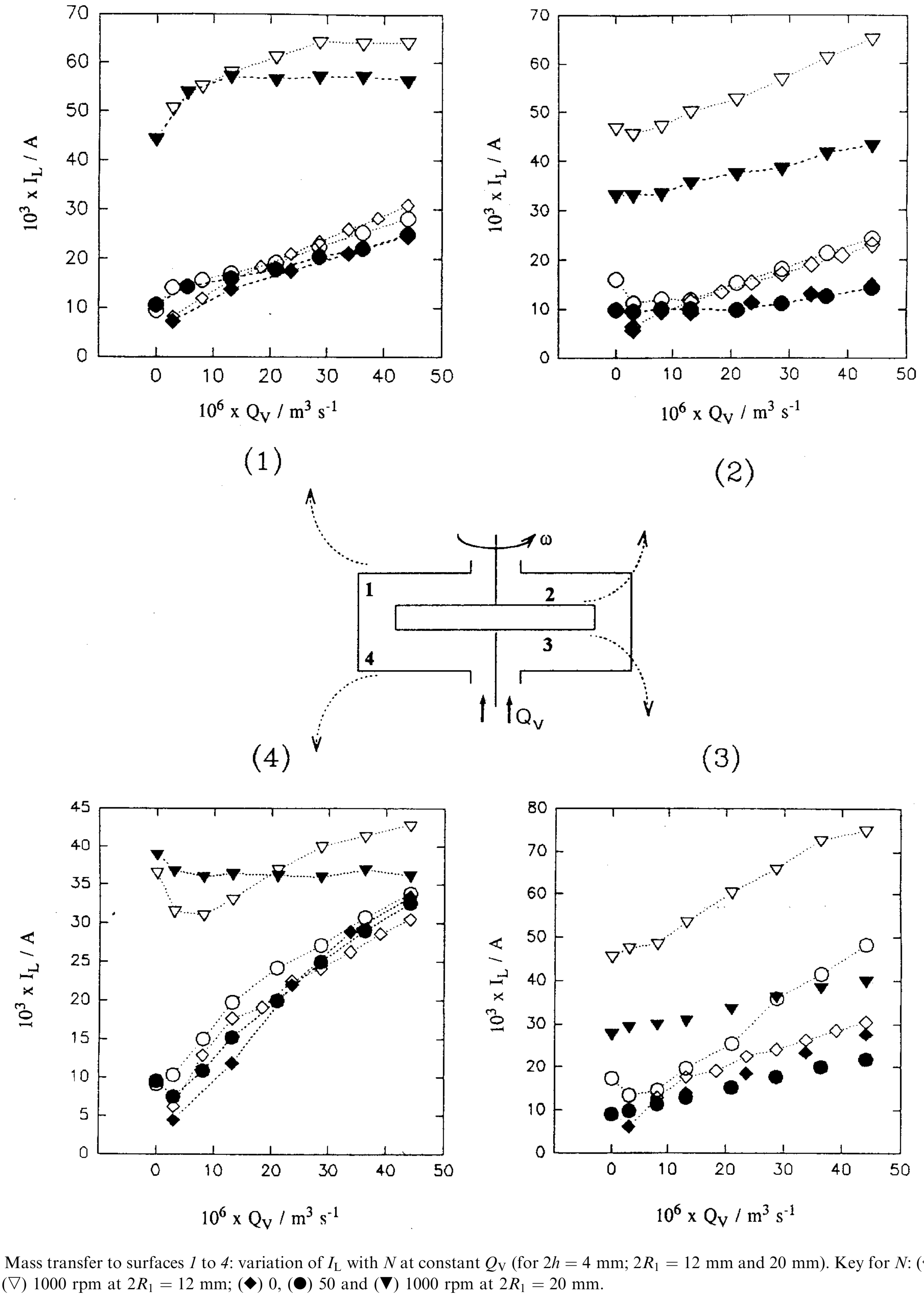

Fig. 4. Mass transfer to surfaces *1* to *4*: variation of I_L with N at constant Q_V (for $2h = 4$ mm; $2R_1 = 12$ mm and 20 mm). Key for N: (◇) 0, (○) 50 and (▽) 1000 rpm at $2R_1 = 12$ mm; (◆) 0, (●) 50 and (▼) 1000 rpm at $2R_1 = 20$ mm.

dence between the exchange surfaces and the data presented.

Analysis of Figures 2 to 5 reveals the influence of different parameters (rotation rate N; volumetric flow rate Q_V; distance $2h$; diameter $2R_1$) on the limiting diffusion current, I_L, at surfaces *1* to *4* although the range of parameters as $2h$ and $2R_1$ is small.

3.1. *Convergent flow region*

3.1.1. *Surface 1*

I_L increases with N at constant Q_V, but the effect of Q_V is greater at small values of N ($N < 200$ rpm). This means that mass transfer depends in this domain on both Q_V and N. Beyond $N = 200$ rpm, mass transfer is controlled

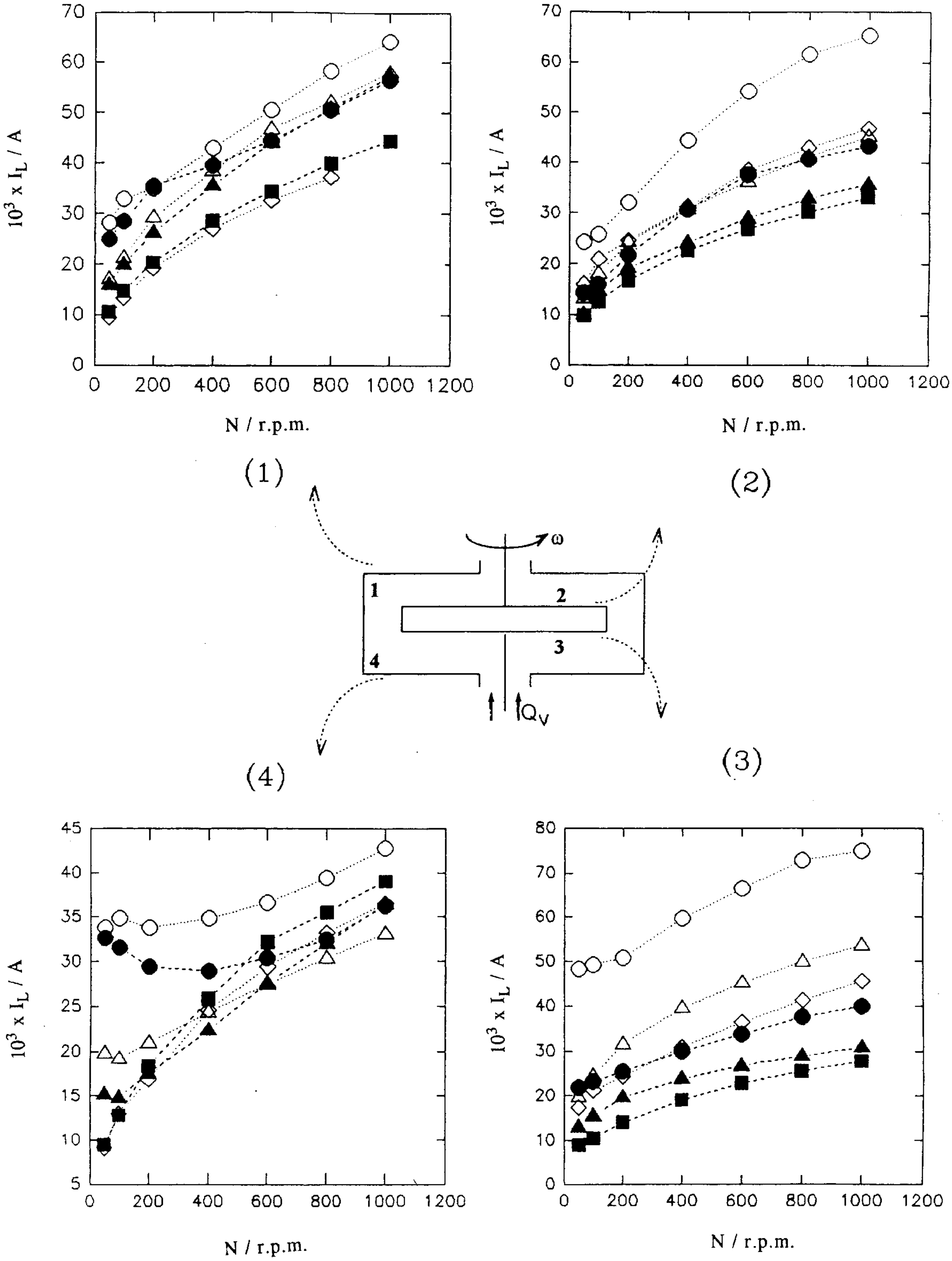

Fig. 5. Mass transfer to surfaces *1* to *4*: variation of I_L with Q_V at constant N (for $2h = 4$ mm; $2R_1 = 12$ mm and 20 mm). Key for Q_V: (◇) 0, (△) 13×10^{-6} and (○) 44×10^{-6} m^3 s^{-1} at $2R_1 = 12$ mm; (■) 0, (▲) 13×10^{-6} and (●) 44×10^{-6} m^3 s^{-1} at $2R_1 = 20$ mm.

by rotation only (I_L becomes rapidly independent of Q_V as Q_V is increased from zero). Figure 3 shows the variation of I_L with Q_V at different values of N for two interdisc gaps: all the other parameters being constant, a decrease in $2h$ improves the transfer. As $2R_1$ was only varied from 12 to 20 mm, a conclusion cannot be drawn concerning its influence (Figures 4 and 5), except that at high Q_V values there is a mass transfer improvement when $2R_1$ decreases.

3.1.2. *Surface 2*

I_L increases with N and with Q_V (Figure 2); the increase is small when $2h$ decreases (Figure 3) whereas a decrease in $2R_1$ leads to an appreciable improvement in I_L

(Figures 4 and 5). As the respective influences of N, Q_V, $2h$ and $2R_1$ on I_L appear to be simple, it can be expected that empirical correlations including these parameters would be easily obtained.

3.2. *Divergent flow region*

3.2.1. *Surface 3*

At a given value of N, the influence of Q_V on I_L is more pronounced than for surface *2* (Figure 2). For $N <$ 200 rpm, the experimental points are few but this domain may correspond to a dominant effect of Q_V. Figures 3 and 4 show that a change of $2h$ from 4 to 8 mm results in mass transfer improvement, especially at small values of N. At a given Q_V, there is a decrease of I_L when $2R_1$ is changed from 12 to 20 mm, and the effect on I_L is more marked as N is high. As indicated above, the observed effects of N, Q_V and $2R_1$ suggest that empirical correlations including these parameters would be easily obtained.

3.2.2. *Surface 4*

I_L increases with N at constant Q_V (Figure 2). However, at constant N, I_L first decreases and then increases when Q_V increases from zero. In other words, the experimental curves I_L against Q_V at constant N present two domains (Figure 3): (i) at low values of Q_V [$Q_V <$ 10 $(\mu\text{m})^3\ \text{s}^{-1}$], where I_L decreases when Q_V increases; and (ii) at higher values of Q_V, where I_L increases with Q_V.

By introducing pumped flow progressively, first the organized structure of the recirculation cells is modified near the entrance of hydraulic diameter $2e$; at higher Q_V values, the cells are compressed against surface *4*.

The presence of a minimum in the variations of I_L with Q_V is also observed when one considers the influence of $2h$ (Figure 3) and that of the entrance diameter $2R_1$ (Figures 4 and 5). The value of I_L obviously results from a competitive influence of Q_V and N: at low rotation velocities, the influence of Q_V is dominant while at high rotation velocities N determines the transfer.

Figure 6(a, b) shows the suggested structures in the divergent and the convergent flow regions respectively, while Figure 6(c) reproduces the simple circulating cell verified in [8].

4. Discussion

4.1. *Transfer at the four surfaces: qualitative comparison*

For surfaces *1* and *4*, the influence of rotation is approximately the same, but the influence of Q_V is different (progressive control by the rotation for surface *1*; combined influence of Q_V and N for surface *4*). The effect of $2h$ and $2R_1$ is comparable for both surfaces.

As for the two sides of the rotating disc (surfaces *2* and *3*), it appears that: (i) the effect of Q_V on the mass transfer is higher at surface *3* than at surface *2*; (ii) the distance $2h$ is a parameter for surface *2*, not for surface *3*; and (iii) at a given Q_V, the mean liquid velocity in the central annular section increases when $2R_1$ is decreased and mass transfer is improved.

These results are qualitatively reminiscent of wall to liquid mass transfer at the cylinders of a Couette–Taylor–Poiseuille flow [3, 4] where two domains were distinguished: first, at low flow rates, where the axial flow renders the mean mass transfer coefficient smaller in comparison with rotation alone. Such a decrease in mass transfer is due to eddies stretched in the direction of axial flow; and second, at higher values of Q_V, where an

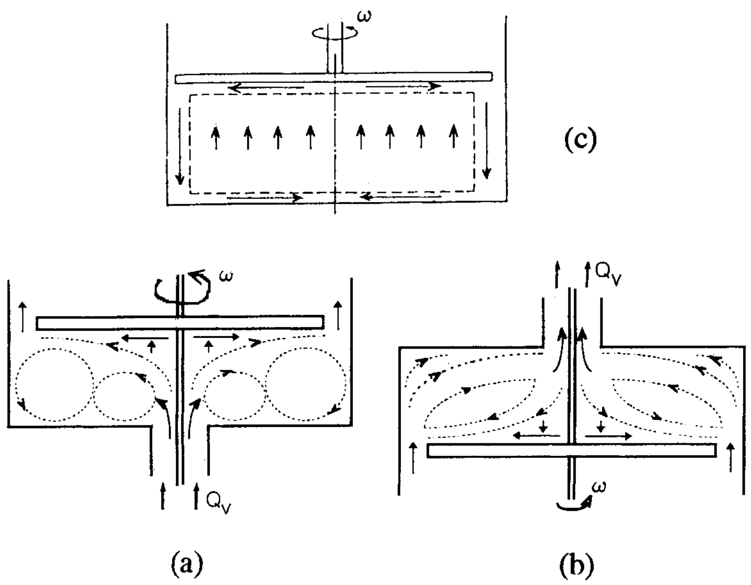

Fig. 6. Suggested flow structures under the combined effect of Q_V and N (schemes (a) and (b)) and structure below a rotating disc in a box (scheme (c)).

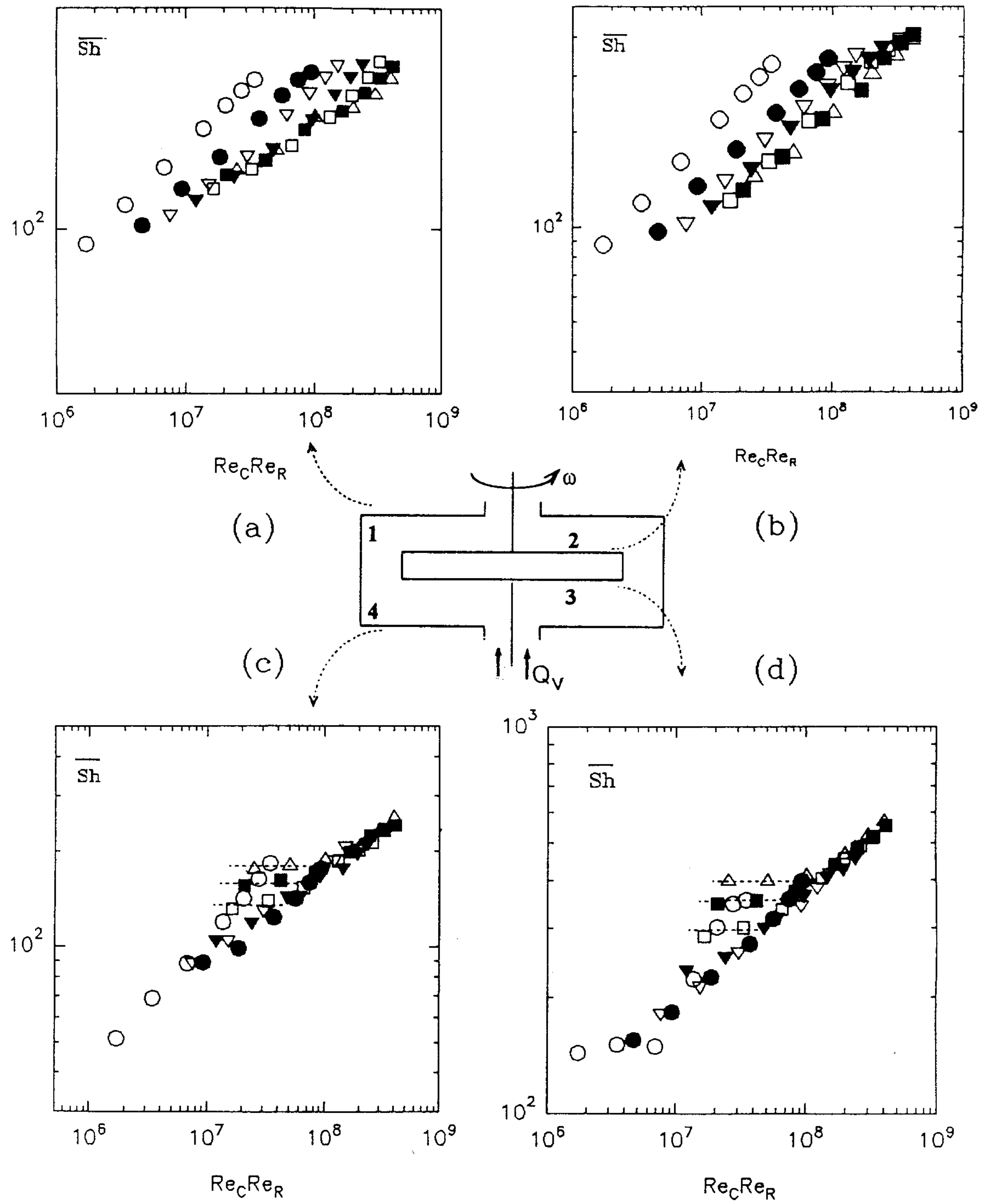

Fig. 7. Variations of $\log(\overline{Sh})$ with $\log(Re_C \times Re_R)$ for surfaces *1* to *4* (for $2h = 8$ mm; $R_1 = 6$ mm; $R_2 = 28$ mm).

increase in Q_V improves mass transfer and is characterized by the presence of eddies of nonuniform size.

For this problem of wall-to-liquid mass transfer in the presence of a Couette–Taylor–Poiseuille flow, empirical correlations proposed for both domains were indicated on an axial Reynolds number against the Taylor number plot.

4.2. *Empirical correlations*

Ashworth [15, 18] correlated empirically mass transfer results expressing $\overline{Sh}$ as a dimensionless function:

$$\overline{Sh} = \left(\frac{H}{R_2}\frac{H^2}{R_2^2 - R_1^2} Re_R Re_C\right)^{\beta}$$

with $\beta = 0.5$ for the stationary disc and $\beta = 0.6$ for the rotating disc. Ashworth [15, 18] put in evidence the difficulty to correlate empirically, in a wider domain, mass transfer results corresponding to each disc. For the complex Couette–Taylor–Poiseuille flow, the flow structure is similar at both cylinders and empirical mass transfer correlations can be obtained in extended hydrodynamical flow regimes. In the present case, not only

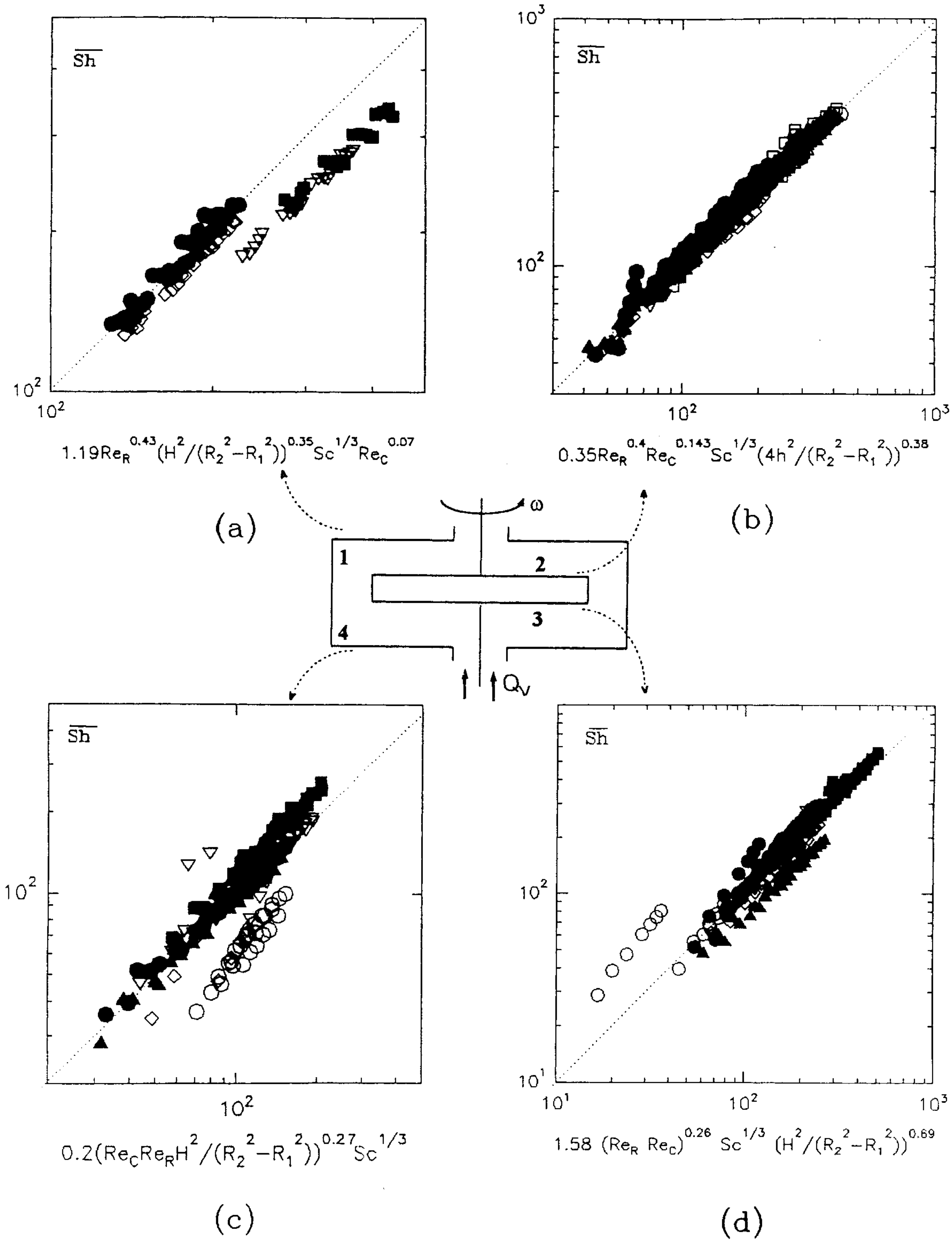

Fig. 8. Empirical correlations for surfaces *1* to *4*.

the flow structure is not the same over the different discs but the experimental parameters exert a much stronger influence on structure.

The Rossby number $Ro = Re_C/Re_R$ permits the distinction between three types of mass transfer control: by forced flow, rotation and mixed control. The current results lead to the following deductions: (i) for $Ro < 0.05$, mass transfer is controlled by rotation, and the empirical correlation would have the form $\overline{Sh} \propto f(Re_R)$; (ii) for $Ro > 1.3$, mass transfer is controlled by forced flow, and $\overline{Sh} \propto f(Re_C)$; (iii) for $0.05 < Ro < 0.5$, mixed control is expected and $\overline{Sh} \propto f(Re_C, Re_R)$, that is, $\overline{Sh} \propto f(Re_C \times Re_R)$ according to the conclusions of Ashworth.

Figure 7 shows bilogarithmic representations of $\overline{Sh}$ against $Re_C \times Re_R$. For surfaces *3* and *4* (Figures 7(d, c)), each short horizontal dotted line corresponds to a given value of Q_V, and is characteristic of a control by forced flow; these dotted lines tend to the straight line $\log \overline{Sh} \propto \log(Re_C \times Re_R)$ which characterizes mixed control. No general correlation taking into account the two types of control could readily be established.

If the data corresponding to mixed control are considered, the final empirical correlations in Figure 8 and summarized in Table 1 are obtained. Note in Figure 8(c, d) that a set of points corresponds to $H/(R_2 - R_1) < 0.1$, very close discs ($H = 2$ mm), and a Rossby number higher than 1.3, a value which characterizes control by forced flow.

In these correlations corresponding to surfaces *3* and *4* under mixed control, the exponent of the product $Re_R \times Re_C$ is 0.26–0.27, even if hydrodynamic conditions near the surfaces are not exactly the same. In contrast, the exponents of the term $H^2/(R_2^2 - R_1^2)$ are different in the two correlations, and they differ from those given by Ashworth [15] for the corresponding terms (Table 1), probably because the hydrodynamic domains explored in [15] and in the present work are different.

In the presence of forced flow only ($N = 0$), it was well established empirically in Part I [1] that mass transfer to surface *3* varies as $Q_V^{0.62}$ and not $Q_V^{0.5}$ similar to mass transfer at a disk impinged by a jet [19]. The results shown in Figure 4 for surface *3* and $N = 0$ establish the influence of the flow rate as $Q_V^{0.57}$ and $Q_V^{0.55}$, respectively, for the two values of $2R_1$. However, comparison with jet impingement is not fully justified, since the entering jet was not only confined but it was also formed around a rod, and it was concluded in [1] that these two particular factors lead to mass transfer improvement.

At surfaces *1* and *2* mass transfer is mainly controlled by rotation. This is well confirmed by the graphical correlations (Figures 8a, b) and by comparison of the exponents of Re_R and Re_C in each correlation shown in Table 1.

At a given value of the product $Re_R \times Re_C$, $\overline{Sh}$ is smaller for surface *4* than for the other three surfaces (Figure 7). This means that limiting mass (or heat) transfer, which has to be considered in the design of a cell depicted by Figure 1, occurs at surface *4*. Unfortunately, owing to the great variation of the exponents in the correlations of Table 1, a graphical comparison of all the correlations cannot be made.

5. Conclusions

Mass transfer between a liquid and disks in a system combining pumped flow and rotation of a category of discs, presents a complex problem which depends on geometrical and hydrodynamic parameters (i.e., flowrate, rotation velocity). Only an empirical analysis of the results is possible, as in the extreme cases of forced flow only and rotation only considered in Part I [1].

At given experimental conditions, the smaller value of the mass transfer coefficient corresponds to the stationary surface (surface *1*) situated in the convergent flow region. This is important because it indicates that surface *1* is mass transfer limiting in the entire cell. In the case of an electrochemical reactor, this also means that the maximum current density to be applied in the cell would be the limiting current density at surface *1*. In the convergent flow region, mass transfer is controlled by rotation while the control is mixed in the divergent flow region. An empirical correlation was established for each of the four surfaces.

Mass transfer studies using microelectrodes in an insulated or conducting wall offer a useful perspective for the investigation of pertinent hydrodynamic flow structures.

Acknowledgements

E. Bezerra Cavalcanti acknowledges receipt of financial support from the CNPq of Brazil. The authors are grateful to Prof. T. Z. Fahidy (University of Waterloo, Canada) for his valued help in improving the English language of the paper.

References

1. E. Bezerra Cavalcanti and F. Cœuret, *J. Appl. Electrochem.* **29** (1999).
2. F. Cœuret and A. Storck, '*Eléments de Génie Electrochimique*' (Tec-Doc Lavoisier, Paris, 1984).
3. F. Cœuret and J. Legrand, *Electrochim. Acta* **26** (1981) 865.
4. J. Legrand and F. Cœuret, *T Can. J. Chem. Eng.* **65** (1987) 237.
5. F.S. Holland, *Chemistry and Industry* **7** (1978) 453.
6. G.A. Ashworth, P.J. Ayre and R.E.W. Jansson, *Chemistry and Industry* **4** (1975) 382.
7. D. Kinnear and P.A. Davidson, *Trans. ASME* **116** (1994) 655.
8. E.B. Cavalcanti and F. Cœuret, *J. Appl. Electrochem.* **26** (1996) 655.
9. M.L. Adams and A.Z. Szeri, *J. Appl. Mech.* **49** (1982) 1.
10. A.Z. Szeri, S.J. Schneider, F. Labbe and H.N. Kaufman, *J. Fluid Mech.* **134** (1983) 103.
11. C. Prakash, U.S. Powle and N.V. Suryanarayana, *AIAA J.* **23** (1985) 1666.
12. F.B. Thomas, P.A. Ramachandran, M.P. Dudukovic and R.E.W. Jansson, *J. Appl. Electrochem.* **18** (1988) 768.
13. J. Peres, Thése de Troisiéme Cycle, University of Poitiers, France (1966).
14. F. Kreith, E. Doughman and H. Kozlowski, *J. Heat Transfer* **85** (1963) 153.
15. R.E.W. Jansson and G.A. Ashworth, *Electrochim. Acta* **22** (1977) 1301.
16. R.E.W. Jansson and R.J. Marshall, *The Chemical Engineer* (1976) 769.
17. J. Groroghchian, R.E.W. Jansson and R.J. Marshall, *Electrochim. Acta* **24** (1979) 1175.
18. G.A. Ashworth, PhD thesis, Southampton University (1977).
19. A. Bensmaili and F. Cœuret, *Int. J. Heat Mass Transfer* **33** (12) (1990) 2743.